

# Enzymatic hydrolysis of different allomorphic forms of microcrystalline cellulose

Diana Ciolacu · Selestina Gorgieva ·  
Daniel Tampu · Vanja Kokol

Received: 19 April 2011 / Accepted: 26 September 2011 / Published online: 8 October 2011  
© Springer Science+Business Media B.V. 2011

**Abstract** This paper investigates the enzymatic hydrolysis of three main allomorphic forms of microcrystalline cellulose using different cellulases, from *Trichoderma reesei* and from *Aspergillus niger*, respectively. It was demonstrated that both the morphological and crystalline structures are important parameters that have a great influence on the course of the hydrolysis process. The efficiency of the enzymatic hydrolysis of cellulosic substrates was estimated by the amounts of reducing sugar and by the yield of the reaction. Changes in the average particle sizes of the cellulose allomorphs were determined during enzymatic hydrolysis. The accumulation of soluble sugar within the supernatant was used as a measure of the biodegradation process's efficiency, and was established by HPLC-SEC analysis. Any modifications in the supramolecular structure of the cellulosic residues resulting from the enzymatic hydrolysis were determined by X-ray diffraction. The action of each cellulase was demonstrated by a reduction in the crystalline index and the crystallite dimensions of the corresponding allomorphic forms. The crystalline structure of allomorphic forms I and II did not suffer

significant modifications, while cellulose III recorded a partial return to the crystalline structure of cellulose I. The microstructures of cellulose allomorph residues were presented using optical microscopy and scanning electron microscopy.

**Keywords** Cellulose allomorphs · Cellulases · Particle size · XRD · HPLC-SEC · SEM

## Introduction

Cellulose, the most abundant polysaccharide on earth is an almost inexhaustible renewable raw material with an expanded role as a source of fuels and commodity chemicals for the future. Throughout industry, the biological conversion of cellulose materials to glucose has proved to be a useful method for obtaining valuable products, such as bioethanol and various chemicals, without competing with food/feed production (Varma 2004).

Cellulose has also been considered recently as an attractive starting material for making nano- and micro-materials with unique physical and chemical properties. Several methods have been proposed on how to prepare and isolate these materials from various resources, involving acid hydrolysis, mechanical treatments (Azizi Samir et al. 2005; Habibi et al. 2010; Das et al. 2010) and more recently enzymatic

---

D. Ciolacu · S. Gorgieva · V. Kokol (✉)  
Institute for Engineering Materials and Design, University  
of Maribor, Smetanova ul. 17, SI-2000 Maribor, Slovenia  
e-mail: vanja.kokol@uni-mb.si

D. Ciolacu · D. Tampu  
“Petru Poni” Institute of Macromolecular Chemistry,  
41A Grigore Ghica Voda Alley, 700487 Iasi, Romania

pretreatments (Paakko et al. 2007; Siqueira et al. 2010; Siró and Plackett 2010).

The enzymatic hydrolysis of cellulose is a complex process which has been studied intensively over the last few decades. However, these studies have generally been oriented towards the physiological characteristics of cellulolytic microorganisms, and also on the biochemical properties of the enzymes synthesized by them (Mansfield and Meder 2003; Russell et al. 2009). The widely-accepted mechanism for enzymatic cellulose hydrolysis suggests that three different types of cellulases work synergistically in a cellulase complex during this process, producing a valuable key intermediate that can be further transformed into various other materials and chemicals (Davies and Henrissat 1995; Lynd et al. 2002; Gusakov et al. 2007): (1) endoglucanases (EG: EC 3.2.1.4) which randomly hydrolyze accessible intramolecular  $\beta$ -1,4-glucosidic bonds in cellulose-chains at internal positions, generating oligosaccharides of various lengths and, consequently, new-chains ends (Liu et al. 2009); (2) exoglucanases (cellobiohydrolases, CBH: EC 3.2.1.91) acting on the chain-termini to release soluble cellobiose or glucose, as major products, and (3)  $\beta$ -glucosidases (BGL: EC 3.2.1.21) which hydrolyze cellobiose to glucose, in order to eliminate cellobiose inhibition (Kumar et al. 2008).

It was also found that the slow reaction and the decreasing rates as the conversion proceeds can be directly related to the cellulose properties (insoluble nature, crystallinity, surface area, porosity, degree of polymerization, etc.), the features of the enzymatic process (deactivation, inhibition, adsorption, processivity, synergy), the mass-transfer (substrate adsorption, bulk and pore diffusion, etc.) and the intrinsic kinetics (Zhang and Lynd 2004; Yeh et al. 2010; MacLellan 2010; Bansal et al. 2010; Karmakar and Ray 2011). However, one cellulose feature that has not yet been investigated refers to the effect of the variety of physical structures adopted by the cellulose macromolecules being in different crystalline forms, on biodegradation. There have only a few studies on the relationship between the fine-structure of cellulose allomorphs and their enzymatic hydrolysis available so far (Weimer and Odt 1995; Pu et al. 2006; Ciolacu 2007; Ciolacu et al. 2007, 2008).

Four major types of cellulose allomorphs have been reported based on X-ray diffraction patterns: celluloses I, II, III, and IV (Ciolacu and Popa 2010a, b). The

natural form of cellulose, so-called cellulose I, is the most important crystalline form of cellulose and the most abundant. It can be found within the major structural components of all plant cell-walls and represents the largest biomass on earth. Furthermore, native cellulose has been found to be a composite of cellulose I $\alpha$  and I $\beta$  crystalline forms (Atalla and VanderHart 1984; Nishiyama et al. 2002, 2003). The cellulose I form can be easily converted into the second crystalline form of cellulose II by regeneration or mercerization processes. The transition from cellulose I to cellulose II is irreversible, and this implies that cellulose II is a stable form as compared with the metastable cellulose I. The other crystalline forms known as cellulose III and cellulose IV can be derived from both cellulose I and II, using different treatments. Thus, cellulose III can be prepared by soaking cellulose samples in anhydrous liquid ammonia at  $-80$  °C or in organic amine (Wada et al. 2004a, 2006), followed by removal of the reagent, while cellulose IV can be obtained from thermal treatments in glycerol at about 260 °C (Wada et al. 2004b).

The allomorphs of cellulose are different from the supramolecular structure point of view, such as the dimensions of monoclinic unit cell, densities of intra- and inter-chain bonds, polarity, and the packing degrees of macromolecular chains. Generally, the crystalline domains of native cellulose are formed almost exclusively from cellulose I, thus the cellulose allomorphs may be considered as analogue substrates, and represent useful materials for testing the hydrolysis mechanism of cellulose at the molecular level (Ciolacu and Popa 2010a). Thus, the aim of this research was to examine the influence of different supramolecular architectures of the allomorphic forms of microcrystalline cellulose (cellulose I, II and III) on their enzymatic hydrolysis, by using endoglucanase enzymes from different fungi, and by analyzing those structural changes occurring during the hydrolysis process.

## Experimental part

### Materials

Three forms of crystalline cellulose were used throughout the study. Avicel PH-101, purchased from Sigma–Aldrich: Fluka, was used as cellulose I—AI. Mercerized cellulose with a crystalline form of

cellulose II (AII) was prepared from microcrystalline cellulose by soaking it in 17.5% NaOH for 24 h at 15° C, followed by washing thoroughly with distilled water and air-dried. Samples with the crystalline form of cellulose III were prepared from microcrystalline cellulose by soaking them in organic amine (100% ethylenediamine) for 24 h at room-temperature, followed by washing with anhydrous methanol, and finally air-dried. Two endo-type cellulases (EC 3.2.1.4) from different sources, *Trichoderma reesei* (C8546,  $\geq 1$  U/mg solid) and *Aspergillus niger* (C1184,  $\geq 0.3$  U/mg solid) were purchased from Sigma–Aldrich. All other chemicals and reagents used were of analytical grade.

## Methods and measurements

### Enzymatic hydrolysis of cellulose

The allomorphs were subjected to enzymatic hydrolyses by comparing the action of two different cellulases, one from *Trichoderma reesei* (*T. reesei*) and one from *Aspergillus niger* (*A. niger*). After pre-swelling of 0.5 g cellulosic substrate in 15 mL 1 M citrate buffer (pH 4.8), 5 mL of enzyme solution with a concentration of 30 U/mL was added. The flask was placed in an incubator at 37 °C and 80 rpm. Samples were withdrawn at different time-periods, namely at 24 h (marked with 1), 48 h (marked with 2), and 72 h (marked with 3), then centrifuged and the supernatant refrigerated. As functions of the type of cellulase used for the enzymatic hydrolysis reaction, the obtained cellulosic residues was marked with “a” for *T. reesei* and with “b” for *A. niger*. The samples were analyzed for any sugar-content reduction by the dinitrosalicylic acid (DNS) method, after appropriate dilution (Miller 1959).

### Particles size and size distribution

The particle size analysis was performed by laser diffractometry (Malvern Particle Mastersizer 2000, Malvern Instruments Ltd., Malvern, UK). This instrument was calibrated with deionized water. All the samples were subjected to sonication for 10 s and stirred at 1,750 rpm to ensure good dispersion in the aqueous medium. All the measurements were done in triplicate and, the average data reported.

### High performance size-exclusion chromatography (HPLC-SEC)

Size-exclusion chromatography was used to evaluate the molecular weights ( $\bar{M}_w$ ) of the degraded products from the enzymatic hydrolysis of cellulose. The analyses were performed using the High Performance Liquid Chromatography System (Agilent Technologies 1200 Series) connected with a Refractive Index detector (RID). PL aquagel-OH column (Agilent Technologies) with dimensions of 300 × 7.5 mm and pore-size 8  $\mu\text{m}$  was used for the determination of  $\bar{M}_w$  compounds. The column's compartment temperature was increased to 40 °C in order to enhance the chromatogram resolution. As the mobile phase, highly-pure Milly Q water from Millipore Systems was used at a flow rate of 1 mL/min. The samples were filtered through a 0.22  $\mu\text{m}$  PVDF membrane filter (Rotilabo–Spritzenfilter) before injection. 20  $\mu\text{L}$  of supernatants were injected into the system and the analysis was carried out for 30 min. Polysaccharide standard with a known molecular weight was used to estimate the calibration curve for determining the sample's molecular weight. HPLC-SEC data were evaluated using CHEM STATION (Agilent Technologies) computer software.

### X-ray diffraction analysis

Wide-angle X-ray diffraction was performed on a Bruker-AXS: D8 ADVANCE apparatus, equipped with a transmission-type goniometer, using Ni-filtered Cu-K $\alpha$  radiation at 40 kV. The goniometer was scanned stepwise every 10° from 10° to 40° within the  $2\theta$  range. The resulting diffraction patterns exhibited peaks which were deconvoluted from a background scattering by using Lorentzian functions, while the diffraction pattern of an artificially amorphized sample was approximated by a Gaussian functions curve fitting analysis (Ciolacu 2007). The structural parameters were calculated using TOPAS 4.2 (Bruker-AXS, Germany) and DIFFRAC.EVA V1.1 (Bruker-AXS, Germany) software.

Estimation of the crystallinity indexes (CrI) of the cellulose samples was established by using the following equation (Sun et al. 2009):

$$\text{Cr.I.} = [\text{Ac}/(\text{Aa} + \text{Ac})] \times 100 (\%) \quad (1)$$

where  $A_c$  is the surface of the crystalline area, and  $A_a$  is the surface of the amorphous area.

The lattice spacings (d-spacings) were calculated using Bragg equation:

$$\lambda = 2d_{hkl} \cdot \sin \theta \quad (2)$$

where  $d_{hkl}$  is the lattice-spacing within one of the crystallographic planes,  $\lambda$  is the X-ray wavelength, and  $2\theta$  is the corresponding Bragg-angle.

The crystallite size was calculated based on the widths of the diffraction patterns, using the Scherrer equation (Krässig 1993):

$$D_{(hkl)} = \frac{k \cdot \lambda}{\beta \cdot \cos \theta} \quad (3)$$

where  $D_{(hkl)}$  is the size of the crystallite (nm),  $k$  is the Scherrer constant (0.94),  $\lambda$  is the X-ray wavelength (0.154 nm), and  $\beta$  is the full-width at half-the-maximum of the reflection  $hkl$ , measured in  $2\theta$ , the corresponding Bragg-angle.

### Optical microscopy

The cellulosic samples were examined using Leica DM 2500 M optical microscope, in polarized light, at room temperature, and a magnification of  $500\times$ .

### SEM analysis

The morphologies of the cellulosic samples were studied by SEM on a FEI QUANTA 200 3D low-vacuum scanning electron microscope. The fibers were coated with gold particles before examination.

## Results and discussion

### Enzymatic hydrolysis

The reaction rates from enzymatic hydrolysis were identified for all three polymorphic forms of microcrystalline cellulose (AI, AII and AIII), under a separate action of *A. niger* and *T. reesei* cellulases, with a concentration of 30 U/mL. The efficiency of enzymatic hydrolysis regarding the cellulosic substrates was estimated by the amount of sugar released into reaction filtrate, and also by the yield during the reaction.

Table 1 presents the concentration values of the reducing sugar, obtained after 72 h of enzymatic

hydrolysis. The highest hydrolysis rate for cellulose II indicates that the chemical modification of cellulose, i.e. treatment with NaOH solution, caused a decrease in crystallinity degree, and thus an implicit increase in the accessibility of the cellulosic substrate, facts which are important factors when controlling a heterogeneous hydrolysis reaction. The values obtained for cellulose III in comparison with cellulose I, confirm the partial reversion of cellulose III to cellulose I, while also retaining a certain disorganized state at the level of the supramolecular structure, thus making it more accessible to enzymatic attack. This could explain the progress of the hydrolysis rate which was higher in case of cellulose III, rather than cellulose I.

The data regarding the yield during the enzymatic hydrolysis reaction of the cellulose allomorphs suggests that the action of the cellulase from *A. niger* was more pronounced compared to the cellulase from *T. reesei*, and that the efficiency of the reaction increased throughout the whole incubation time, from 24 to 72 h. The most affected substrate was cellulose II, whose yield values were between 54 and 62% in the case of *T. reesei* cellulase, and between 68 and 84% for *A. niger* cellulase. Cellulose I was the least affected, where for the treatment with *T. reesei* cellulase obtained a yield from the reaction of between 6 and 10%.

The influence of the cellulase type on the progress of an enzymatic hydrolysis reaction (Fig. 1), being reflected by the concentration values of the reducing sugars, indicated that the action of *A. niger* cellulase was more evident than the *T. reesei* cellulase. In the case of the cellulose allomorphs hydrolyzed in the presence of *T. reesei* cellulase, the rate of enzymatic degradation was higher during the first 24 h, after which it remained constant. An explanation for this behavior is that during enzymatic degradation, the cellulolytic enzymes attacked more of the amorphous fraction of the substrate. Accordingly, during the progress of the hydrolysis, the rate of reaction decreased as a result of the presence of the crystalline fraction, being more resistant to the cellulase action. Irreversible adsorption or non-specific binding of cellulases can be present besides the thermal inactivation of enzymes (Mussatto et al. 2008). On the other hand, a slower degradation rate of the cellulose allomorphs was recorded with *A. niger* cellulase over the first 24 h of incubation compared to *T. reesei*

**Table 1** Enzymatic hydrolysis of cellulose allomorphs

Cellulose allomorph	Type of cellulase	Total sugars <sup>a</sup> (g/L)	$\eta^b$ (%)		
			24 h	48 h	72 h
AIa	<i>Trichoderma reesei</i>	1.412	6	8	10
AIIa		1.671	54	60	62
AIIIa		1.495	17	18	18
AIb	<i>Aspergillus niger</i>	1.600	21	37	43
AIIb		1.850	68	70	84
AIIIb		1.740	19	31	37

<sup>a</sup> Determined on the basis of the dinitrosalicylic acid (DNS) method

<sup>b</sup> Calculated on the basis of substrate dry weight before and after hydrolysis

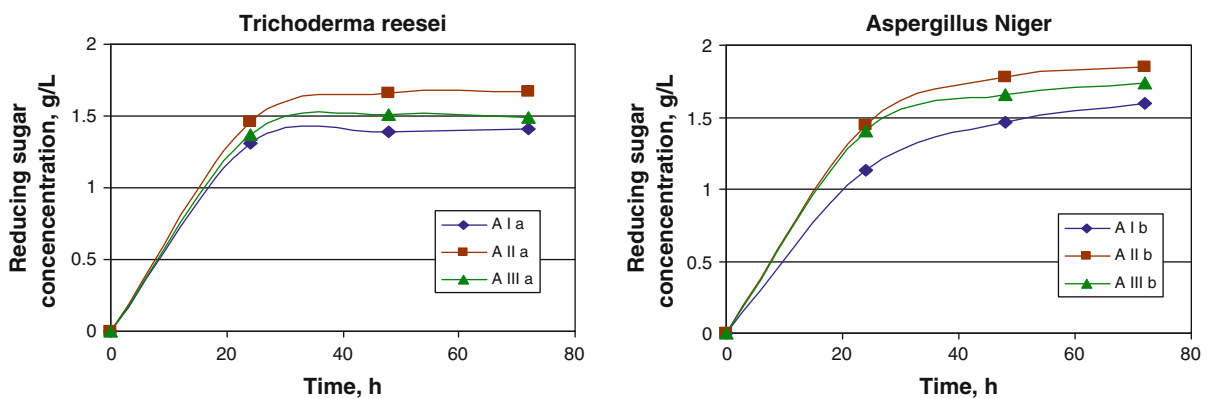


**Fig. 1** The progress of enzymatic hydrolysis regarding different cellulose allomorphs using different cellulases

cellulase, but after 24 h of incubation *A. niger* cellulase exhibited higher cellulolytic activity on all three cellulose allomorphs tested by a continued increase in the reaction rate. An explanation could be the fact that *T. reesei*-strain is deficient in  $\beta$ -glucosidase, which is essential for converting cellobiose into glucose, while *A. niger* has proved to be a very good producer of this, although, based on the enzyme producer data, endo-glucanases should be the main enzymes in the products. However, looking generally,  $\beta$ -glucosidase causes deglycosylation of the substrates and produces gentiobiose, which is a strong inducer of cellulases. Thus, the main product of the hydrolysis with *T. reesei* would be cellobiose, which is a strong inhibitor of endo- and exo-glucanases, and the accumulation of cellobiose would significantly slow-down the overall hydrolysis process (Ahamed and Vermette 2008). The similar behaviour, regarding the fact that *A. niger* cellulase is more efficient than *T. reesei*, was emphasized by

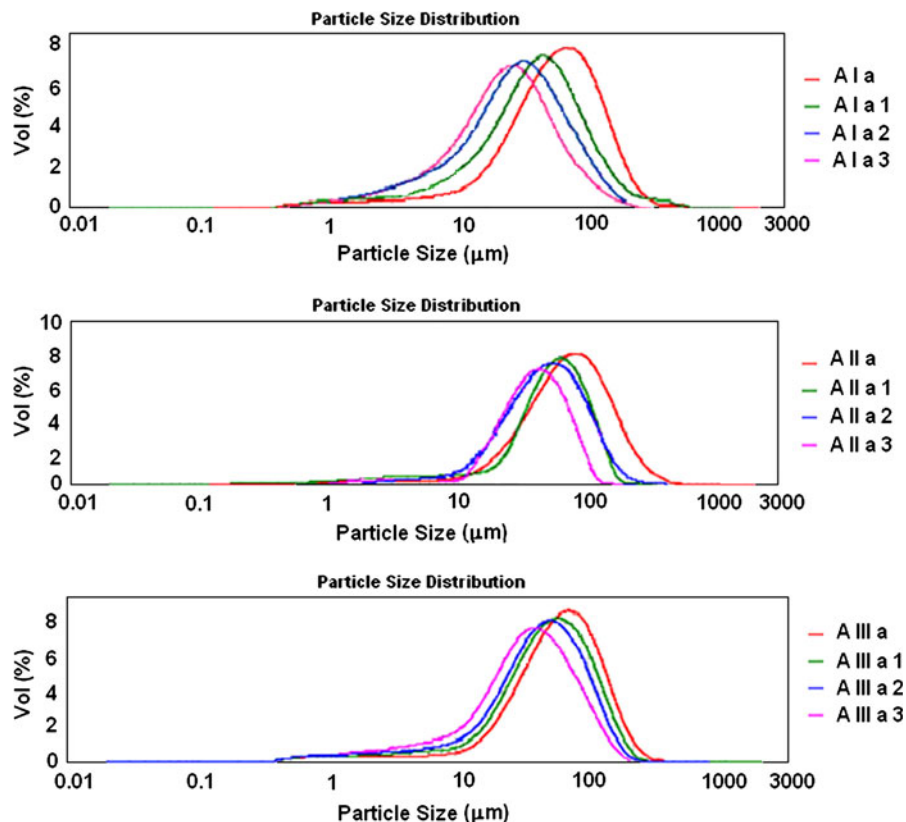
Al-Zuhair (2008) using carboxymethylcellulose and wood-chips as cellulosic substrates.

A strong chemical modification of cellulosic substratum was shown by taking into account the structural differences of the allomorphic forms of cellulose, which led to a decrease of crystalline region, permitting an increase in the hydrolysis rate. The fact that the allomorphic form of cellulose II presented a higher hydrolysis rate than cellulose I is explained by the differences which appeared in the intra- and intermolecular bonds of supramolecular structure for each type of allomorph. As was previously shown, the values obtained for the biodegradation rate of cellulose III reflect a partial reversal to the crystalline form of cellulose I.

#### Particle-size distribution

The effect of enzymatic hydrolysis was also studied by particle-size distribution (PSD) and it was observed

**Fig. 2** Particle size distribution for untreated cellulose allomorphs, and those treated with *T. reesei* cellulase



that modifications depend on both the supramolecular structures of cellulose allomorphs and the activities of the cellulases (Figs. 2, 3).

During enzymatic hydrolysis reaction, the cellulosic allomorphs were cut into small particles, and the quantities of these increased with any increase in incubation time. By comparing the enzymatic degradation of cellulose I using both cellulases, a decrease in particle dimensions could be observed, which was higher for *A. niger* cellulase (between 54.96  $\mu\text{m}$  for AI and 17.8  $\mu\text{m}$  for AI b3), than for *T. reesei* cellulase, being 20.50  $\mu\text{m}$  for AI a3.

Figure 4 presents the changes in the average particle sizes of the cellulose allomorphs along the enzymatic degradation, in the presence of both cellulases. It can be identified that the supramolecular structures of the cellulose allomorphs have different influences on the courses of their enzymatic degradations. The most remarkable size-reduction was recorded for cellulose II, which suffered a decrease in the average diameter of its particles, of 68% in the presence of *A. niger* cellulase and of 62% for *T. reesei* cellulase. Generally, the average diameters of cellulose allomorphs decrease

monotonically with any increase in the enzymatic hydrolysis time, and these samples usually exhibit a bimodal particle size distribution.

#### High-performance size exclusion chromatography

As presented, the enzymatic degradation of cellulose allomorphs is accompanied by the release of soluble sugars, which may consist of a significant amount of glucose, as well as other degradation products, such as cellobiose, cellotriose, etc. (Zhang and Lynd 2004). The accumulation of soluble sugar in the supernatant was used as a measure of the enzymatic hydrolysis process efficiency. Thus it was observed an increase in the hydrolytic efficiency with the reaction time.

Figure 5 shows typical SEC chromatograms of the degradation products obtained after the enzymatic hydrolysis of cellulose II, at different reaction times, using *A. niger* cellulase. This example was selected because in the presence of this cellulase, cellulose II recorded the highest concentration of reducing sugars, compared to the other cellulose allomorphs. The chromatograms show a peak corresponding to higher



**Fig. 3** Particle size distribution for untreated cellulose allomorphs, and those treated with *A. niger* cellulase

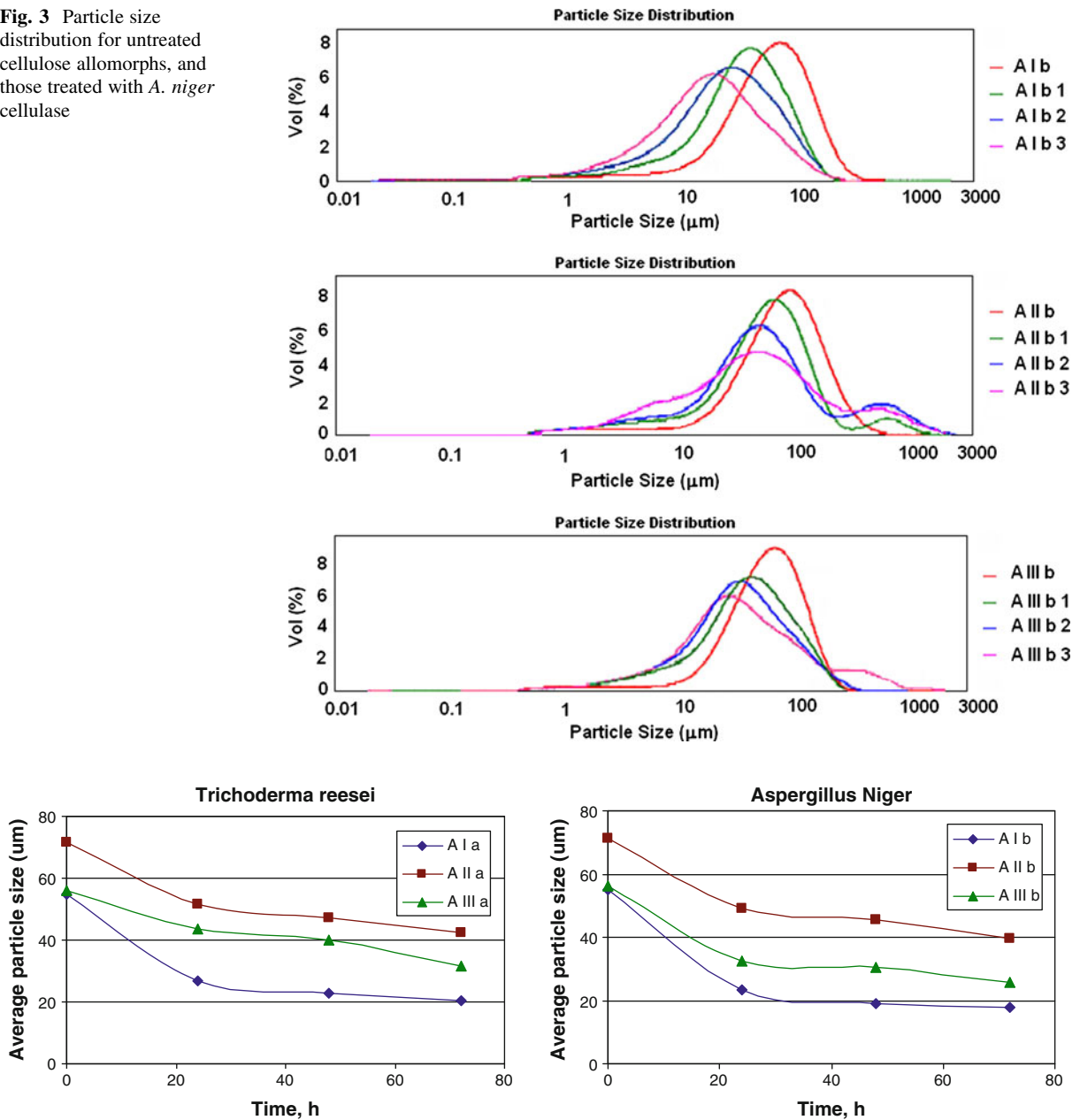


**Fig. 4** The influence of enzymatic hydrolysis time on particle size distribution for studied cellulose allomorphs

$\bar{M}_w$  fractions (retention time between 14 and 16 min) and a main peak in the time interval between 18 and 20 min, corresponding to oligomeric fragments (in this case, glucose). The other peaks, which appear between 16 and 17 min, corresponding to cellotriase (peak 3) and cellobiose (peak 4) are shown in Tables 2 and 3. Comparing the data regarding the areas recorded for the main peak (at a retention time of

around 18 min) with the other ones, it can be also observed that the higher the reaction time, the higher the extension of enzymatic hydrolysis.

The supramolecular structure of cellulose allomorphs has an important effect on the hydrolysis reaction. Thus, the highest quantity of glucose (peak 5) was recorded for cellulose II. The next allomorphic substrate able to degrade is cellulose III, followed by

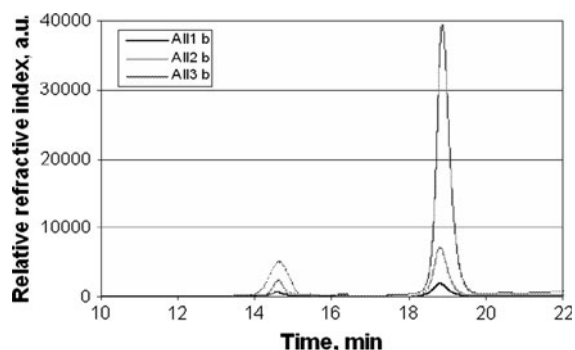


**Fig. 5** HPLC-SEC analysis of those degradation products released upon the hydrolysis of cellulose II in the presence of *A. niger*

cellulose I. The explanation for this behaviour is the reversibility of cellulose III to I, with the maintaining of a more relaxed structure, thus permitting a better digestion of this cellulosic substrate. The obtained data

are in good correlation with those regarding the reducing sugar concentrations.

Taking into account the whole values from Tables 2 and 3, it can be observed that important differences appeared in the peak areas with respect to the  $\bar{M}_w$  and the retention-time. The characteristic retention-times were successfully identified for each type of cellulase which appeared between 14 and 15 min and for glucose which appeared between 18 and 20 min (spectra not shown). An average molecular mass ( $\bar{M}_w$ ) of 76 kDa was found for *A. niger* cellulase (Table 3), while for *T. reesei* a molecular weight of 50 kDa (Table 2) being within the range reported for this cellulase,  $\bar{M}_w$  of 46–52 kDa (Lyagin et al. 2011). The molecular weight of glucose obtained from enzymatic hydrolysis of cellulose allomorphs was 180 Da, and all the intermediary peaks corresponding to different cello-oligosaccharides (cellobiose,

**Table 2** The retention times and the areas of the main peaks determined from HPLC-SEC analysis of the solutions obtained after treatment of cellulose allomorphs with *T. reesei* cellulase

Samples treated with <i>T. reesei</i> cellulase	Area (%)				
	Peak 1	Peak 2	Peak 3	Peak 4	Peak 5
Retention time (min)	14.82	15.38	16.46	17.74	18.84
AI1a	55.32	–	0.34	6.64	37.67
AI2a	36.89	–	3.07	7.56	52.46
AI3a	33.21	–	5.62	–	61.16
AII1a	–	–	44.32	–	55.66
AII2a	–	–	35.56	–	57.57
AII3a	–	–	33.56	–	61.36
AIII1a	–	–	49.37	1.36	49.27
AIII2a	–	–	36.65	–	56.78
AIII3a	–	–	31.93	–	59.92

**Table 3** The retention times and the areas of the main peaks determined from HPLC-SEC analysis of the solutions obtained after treatment of cellulose allomorphs with *A. niger* cellulase

Samples treated with <i>A. niger</i> cellulase	Area (%)				
	Peak 1	Peak 2	Peak 3	Peak 4	Peak 5
Retention time (min)	14.7	15.16	16.35	17.16	18.84
AI1b	29.02	–	1.79	2.07	67.11
AI2b	27.32	–	–	4.58	68.08
AI3b	26.78	–	–	–	70.48
AII1b	32.22	–	–	–	67.77
AII2b	27.52	–	1.69	–	70.77
AII3b	24.24	–	–	–	72.90
AIII1b	31.47	–	–	–	68.52
AIII2b	–	–	30.47	–	69.51
AIII3b	–	–	18.35	–	70.77



cellotriose, etc.) obtained after enzymatic degradation of cellulosic substrates. Thus the obtained data for each cellulose allomorph indicated a decrease in the cellulase content and an increase of the glucose content in the reaction mixture, during the enzymatic hydrolysis process. Moreover, a lot of peaks were observed in the chromatograms recorded for *T. reesei* cellulase corresponding to oligomeric fragments, instead of *A. niger* cellulase where higher peaks were detected corresponding to cellulase (peak 1) and glucose (peak 5). This observation sustains the conclusion regarding the different actions of each cellulase on the cellulosic substrates, as explained previously, i.e. that *A. niger* cellulase exhibited higher cellulolytic activity on cellulose allomorphs than *T. reesei*.

### X-ray diffraction

Deconvolution of the peaks using a soft PeakFit 4.11 was performed in order to identify the structural modifications suffered by the allomorphic forms of microcrystalline cellulose during the process of enzymatic hydrolysis.

X-ray diffractograms of the residues obtained after enzymatic degradation of cellulose I (Fig. 6) show an important decrease of the characteristic crystal lattice with the maximum intensity at (020) found in diffractograms at a Bragg-angle of  $22^\circ$ , as well as intensities of (101) and (10 $\bar{1}$ ) lattice diffractions at  $14^\circ$  and  $16^\circ$ , respectively. This fact indicates a decrease of the crystallinity index of the samples while maintaining the crystalline form characteristic of cellulose I. In regard to the enzymatic hydrolysis in the presence of *T. reesei*, the reduction in intensities of the peaks were more remarkable than those treated with *A. niger*, for cellulose I.

In the case of cellulose II (Fig. 7), the diffractograms confirmed the preservation of the crystalline structure of cellulose II after the cellulase action. However, more important modifications appeared at the intensity of the characteristic crystallographic peaks and implicitly in the crystalline index for cellulose II treated with *T. reesei* cellulase. If the modifications observed in the diffractograms of the allomorphic forms of cellulose I and II was not exactly dramatically, a partial reversibility was observed of cellulose III to the cellulose I (Fig. 8).

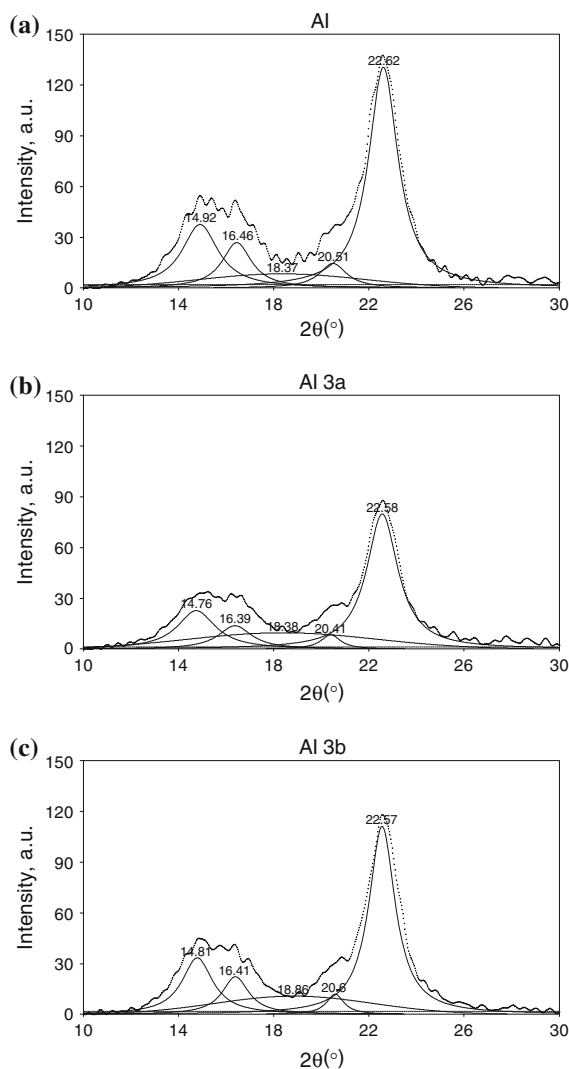


**Fig. 6** X-ray diffraction profiles of cellulose I, untreated (a) and treated with cellulases from *T. reesei* (b) and *A. niger* (c) for 72 h

Generally, the diffractogram of cellulose III contain a peak (101) of around  $11^\circ$ , while the peaks at (10 $\bar{1}$ ) and (002) are superimposed at a Bragg-angle of  $21^\circ$ . The transformation of microcrystalline cellulose to cellulose III is incomplete in the present case. However, in the diffractograms of the residues obtained after the enzymatic hydrolysis of cellulose III, the reflection of plane (101) appeared at approximately the same value for the untreated as well as for the enzymatically-treated cellulose. Instead, near the characteristic peak at (002) another reflection of the plane (002) appeared at higher values for the  $2\theta$  angle,

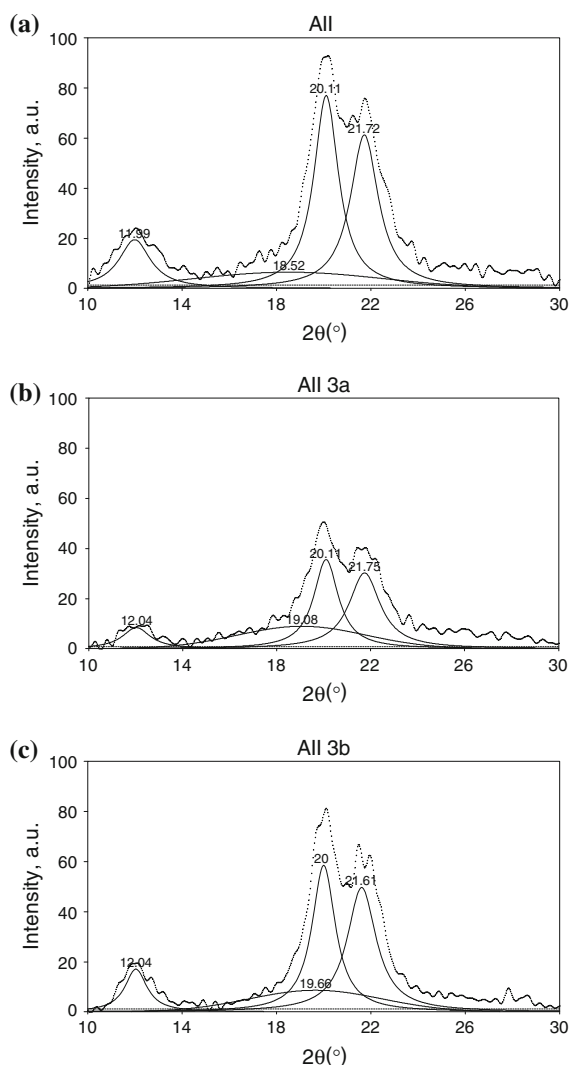


**Fig. 7** X-ray diffraction profiles of cellulose II, untreated (a) and treated with cellulases from *T. reesei* (b) and *A. niger* (c) for 72 h

and characteristic for cellulose I (at  $22^\circ$ ). The presence of peaks at (101) and (10 $\bar{1}$ ) as characteristic for cellulose I, were also clearly in evidence, which appeared at Bragg-angles of  $14^\circ$  and  $15^\circ$ . These observations confirmed the partial reversion of cellulose III to cellulose I and led us to assume that there is a juxtaposition for the reflection of the (002) plane of cellulose III with that of cellulose I. An explanation for this reversibility is the presence of a water-based medium over a long period of time. This characteristic of the allomorphic form of cellulose III is generally known, which implied only a partial recrystallization,

the crystals remained mainly within the distortion and fragmentation (Ciolacu and Popa 2010a, b).

Tables 4 and 5 present those changes that took place during the enzymatic treatment of the cellulose allomorphs, regarding the crystallite dimension (D), lattice spacing (d-spacings), and the crystalline index (CrI). A stronger action of *T. reesei* cellulase against *A. niger* cellulase on the cellulosic substrates can be observed in terms of decreased crystallinity. An explanation of the differences which appear between these two enzymes is the fact that *T. reesei* cellulase hydrolyzed more the amorphous part, while *A. niger* cellulase simultaneously degraded the crystalline and amorphous areas. The obtained data regarding the concentration of reducing sugar, discussed previously, supports this conclusion.

Generally, the X-ray diffraction pattern of cellulose I represents three equal reflections as (101), (10 $\bar{1}$ ) and (002), have many reflections on the layer-lines and two reflections (020) and (040) on the meridian (Hu and Hsieh, 1996). The first three peaks appeared at approximately  $14^\circ$ ,  $16^\circ$ , and  $22^\circ$ , respectively, the peak at about  $20^\circ$  corresponding to the (021) reflection, whereas the (040) reflection is at about  $34^\circ$  (Fig. 6). Four distinct and independent reflections were observed in the case of cellulose II, at (101), (10 $\bar{1}$ ), (002), and (040), which were located at Bragg-angles of  $11^\circ$ ,  $20^\circ$ ,  $21^\circ$ , and  $34^\circ$ , respectively. By transformation from cellulose I to cellulose III, the diffraction pattern modified and, in this case, the reflection at (101) was now at  $11^\circ$ , while the reflections at (10 $\bar{1}$ ) and (002) overlapped at  $21^\circ$ .

Calculation of those crystallite dimensions normal to the hkl planes was come out based on the estimation of the peak width at half-the-maximum amplitude. The crystallite dimensions of four main equatorial reflections were determined and within these, (101), (10 $\bar{1}$ ) and (002) were measured for crystallite width, while the reflection at (040) indicated the crystallite length. The (040) reflection was used to measure the lateral length of the cellulosic samples because this occurs in a direction orthogonal to the longitudinal direction of the microfibril (Garvey et al. 2005).

An increase from cellulose I to cellulose II and III, respectively, was recorded in the case of the crystallite size of untreated cellulose allomorphs along the (10 $\bar{1}$ ) direction, while for the sizes along the other directions, at (101) and (002), a decrease in the dimensions of the

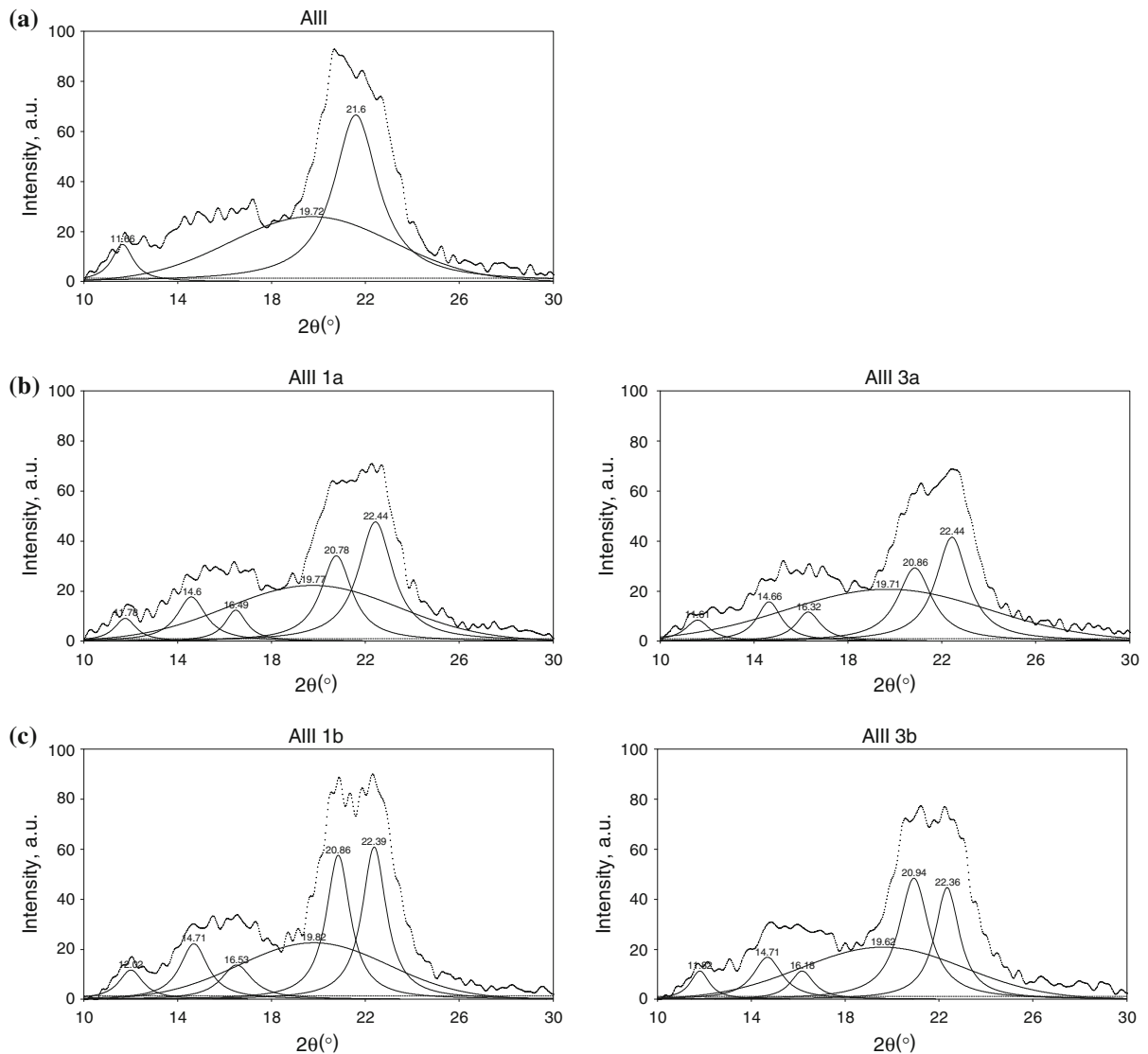


**Fig. 8** X-ray diffraction profiles of cellulose III, untreated (a) and treated with cellulases from *T. reesei* (b) and *A. niger* (c) for 24 h (1) and 72 h (3)

same order was shown. A relationship between the crystallinity index and the crystallite dimensions was observed for the enzymatically-treated cellulose allomorphs, namely, the lower the CrI of the sample, the smaller the obtained dimensions of the crystallite. Only for the apparent crystallite size of the (040) peak was recorded a slight increase in the dimension, with an increase in the hydrolysis reaction time. Sun et al. (2009) also reported an increase in the crystallite dimension at the reflection (040) accompanied by a decrease in the dimensions for the other main

reflections during the process of microcrystalline cellulose conversion into fermentable glucose, within the formic acid reaction system.

The d-spacing of the (101), (10 $\bar{1}$ ), (002) and (040) peaks for each diffractogram were calculated using Bragg's equation. Taking in account all cellulose allomorphs, cellulose I presented smaller d-spacing compared to cellulose II and cellulose III. Based on the literature, the smaller d-spacing in cellulose I indicates a stronger hydrophobic interaction (Wada et al. 2010). In addition, the hydrophobic attraction would act as a

**Table 4** X-ray diffraction parameters of untreated cellulose allomorphs and treated with *T. reesei* cellulase

Samples	Time (h)	D <sup>a</sup> (nm)				d-spacing <sup>b</sup> (Å)				CrI <sup>c</sup> (%)
		(101)	(10 $\bar{1}$ )	(002)	(040)	(101)	(10 $\bar{1}$ )	(002)	(040)	
AI	0	5.3	5.2	8.8	8.3	5.94	5.33	3.90	2.61	87
AI1a	24	5.4	5.7	8.2	9.7	5.90	5.29	3.93	2.61	84
AI2a	48	4.9	5.0	7.2	9.6	5.97	5.31	3.91	2.62	79
AI3a	72	4.3	4.8	8.2	9.8	6.05	5.32	3.90	2.61	76
AII	0	5.1	7.5	8.5	8.6	7.50	4.41	4.10	2.60	85
AII1a	24	5.3	7.5	8.3	12.1	6.92	4.46	4.06	2.60	80
AII2a	48	4.8	7.0	8.7	14.2	7.22	4.43	4.13	2.58	72
AII3a	72	4.0	6.5	7.5	13.6	7.57	4.01	4.01	2.52	63
AIII	0	4.0	8.2	8.2	9.5	7.58	4.26	4.26	2.64	59
AIII1a	24	4.5	7.8	7.8	10.2	7.34	3.93	3.93	2.65	64
AIII2a	48	3.9	8.5	8.5	12.3	7.25	3.91	3.91	2.62	63
AIII3a	72	3.6	7.4	7.4	13.2	7.33	3.92	3.92	2.68	60

<sup>a</sup> Crystallite size perpendicular to the direction of each plane

<sup>b</sup> d-spacing of typical three equatorial peaks of cellulose

<sup>c</sup> Crystalline index

**Table 5** X-ray diffraction parameters of untreated cellulose allomorphs and treated with *A. niger* cellulase

Samples	Time	D <sup>a</sup> (nm)				d-spacing <sup>b</sup> (Å)				CrI <sup>c</sup> (%)
		(101)	(10 $\bar{1}$ )	(002)	(040)	(101)	(10 $\bar{1}$ )	(002)	(040)	
AI	0	5.3	5.2	8.8	8.3	5.94	5.33	3.90	2.61	87
AI1b	24	5.3	4.7	7.6	12.4	6.01	5.33	3.91	2.63	85
AI2b	48	6.3	5.1	7.0	14.7	6.03	5.42	3.93	2.60	82
AI3b	72	4.8	4.5	8.4	14.6	6.01	5.38	3.91	2.62	80
AII	0	5.1	7.5	8.5	8.6	7.50	4.41	4.10	2.60	85
AII1b	24	5.2	7.6	9.7	15.0	7.36	4.48	4.07	2.62	83
AII2b	48	5.0	8.4	7.5	16.1	7.31	4.46	4.04	2.63	81
AII3b	72	5.1	6.8	6.7	16.8	7.31	4.47	4.07	2.60	78
AIII	0	4.0	8.2	8.2	9.5	7.58	4.26	4.26	2.64	59
AIII1b	24	4.3	8.2	8.2	14.5	7.29	4.28	4.28	2.64	58
AIII2b	48	5.3	8.0	8.0	14.9	7.50	4.27	4.27	2.56	55
AIII3b	72	3.7	5.5	5.5	14.7	7.46	3.95	3.95	2.55	53

<sup>a</sup> Crystallite size perpendicular to the direction of each plane

<sup>b</sup> d-spacing of typical three equatorial peaks of cellulose

<sup>c</sup> Crystalline index

main factor for resisting enzymatic hydrolysis by cellulase, while hydrogen-bonds in the first layer of cellulose crystallites could become unstable in water. Thus, this modification from cellulose I to cellulose II and III, respectively, which has weaker hydrophobic interaction, could enhance the hydrolysis rate by

cellulolytic enzyme, observation which is in agreement with the data achieved during this study. The obtained values showed a very slight decreasing tendency for the main reflections, (101), (10 $\bar{1}$ ) and (002), while the data remained the same for (040). Similar observations have been reported in literature (Hayashia et al. 1997).

## Optical microscopy

Microscopic photographs with magnifications of 500× were performed for the untreated microcrystalline cellulose and for those treated with *T. reesei* (AIa 3) and *A. niger* (AIb 3) cellulases, over 72 h (Fig. 9). The micrographs of the cellulosic samples showed a

decrease in the fibers dimensions with any increase in the enzymatic hydrolysis time. The effect of particle reduction is more evident in the presence of *A. niger* cellulase, being already shown to have a much more powerful action on cellulose substrate than *T. reesei* cellulase, which exhibited the most serious shape deformation caused by fiber damages.

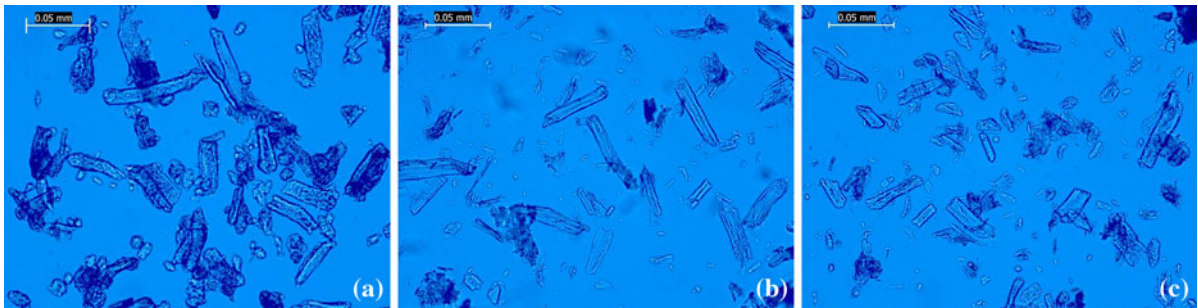


**Fig. 9** Microscopic aspects of initial microcrystalline cellulose, untreated (a) and treated with cellulase from *T. reesei* (b) and *A. niger* (c) for 72 h

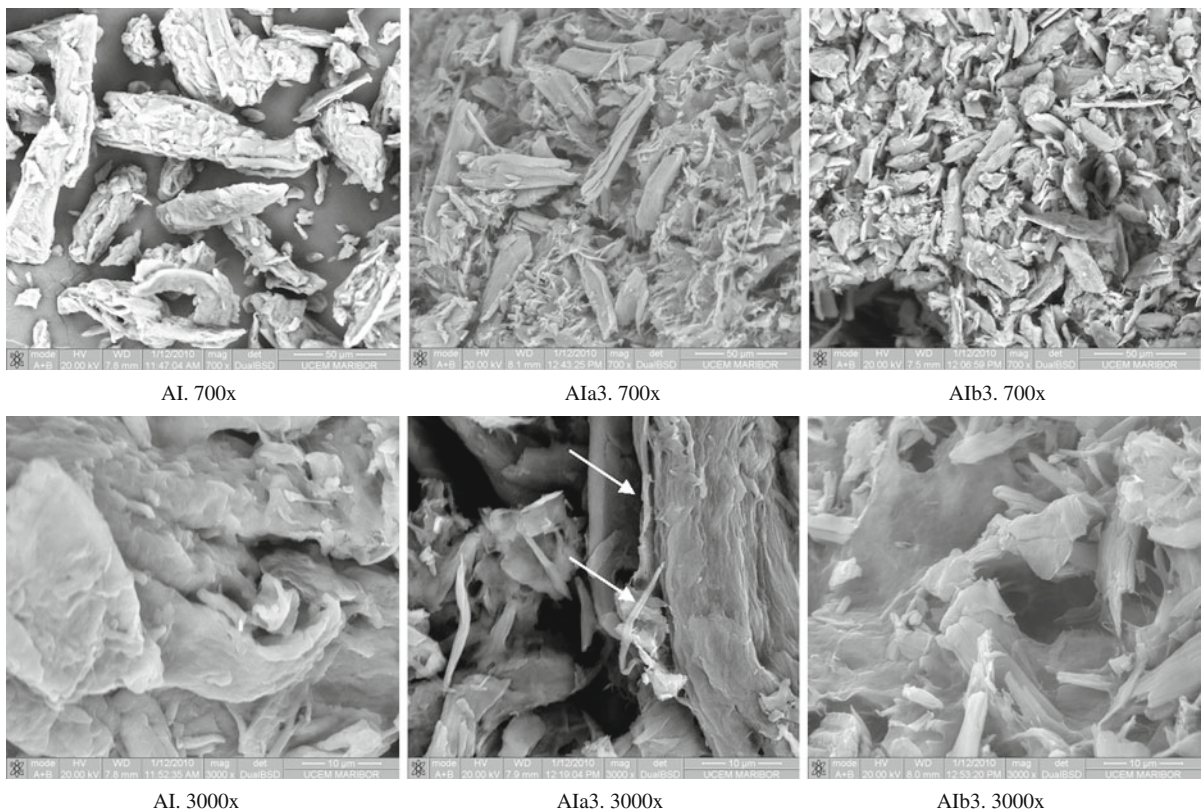


**Fig. 10** SEM images of initial microcrystalline cellulose, untreated (AI) and treated with cellulases from *T. reesei* (AIa3) and *A. niger* (AIb3) for 72 h



## Scanning electron microscopy (SEM)

Supramolecular structural changes in the untreated and differently-treated microcrystalline cellulose were observed using a scanning electronic microscope (SEM). The SEM images presented in Fig. 10 clearly show the morphological differences between the native cellulose and that treated with *T. reesei* or *A. niger* cellulases over 72 h.

The initial particle of microcrystalline cellulose appears fibrous and bulky. After 72 h of enzymatic hydrolysis the dimensions of the particle became lower and thinner. This aspect was more evident in the case of cellulose treated with *A. niger* cellulase, where the particle had the smallest dimension. The cellulosic fragments and breaks along the cellulosic fibers could be observed at a magnification of 700× (A1b3), which meant that the cellulase broke enough glucosidal bonds to weaken the microfibril surfaces and caused splitting. In the case of cellulose treated with *T. reesei* (A1a3), individual microfibrils could be identified at a magnification of 3000x, as a result of the cellulase action.

## Conclusion

The effects of cellulose polymorphism on its biodegradability were evaluated using cellulases from different fungus, *T. reesei* and *A. niger*. It was observed that the hydrolysis rate of cellulose to reducing sugars was more evident for the crystalline structure of allomorphic forms II. Beside, in the presence of aqueous media, cellulose III suffered a partial return to the crystalline structure of cellulose I, the fact which could explain the slower progress of enzymatic degradation rate in comparison with cellulose II.

HPLC-SEC results confirmed the accumulated amount of glucose and other degradation products, being consequently used as a measure of the enzymatic reaction efficiency. During the enzymatic hydrolysis, the scissions of the cellulosic macromolecular chains were evidenced by different modifications in the particle sizes of obtained celluloses, suggesting that the process depends on the supramolecular structures of the cellulose allomorphs and the activities of the cellulases.

Cellulose II was the most affected substrate, which suffered a decrease in the particle average diameter of

68 and 62%, in the presence of *A. niger* and *T. reesei* cellulase, respectively, being related to the difference in hydrolytic actions of cellulases; *T. reesei* hydrolyzes mainly the amorphous part, while *A. niger* simultaneously degrades the crystalline and amorphous areas.

Moreover, a decrease in the crystallinity index and the crystallite dimensions, evaluated by the X-ray diffraction of the enzymatically-treated allomorphs, proves the hydrolytic chain degradation. The microscopic investigation of cellulose allomorphs emphasizes all the statements by showing a decrease in the fiber dimensions with an increase of the enzymatic hydrolysis time. The results of this study generate the hypothesis that the enzymatic hydrolysis process could expand the possibilities for the synthesis of new cellulosic materials with controlled structure–function relationships.

**Acknowledgments** This research was supported by the Marie Curie Transfer of Knowledge Fellowship of the EC FP6 under the contract nr. MTKD-CT-2005-029540-POLYSURF.

## References

- Ahamed A, Vermette P (2008) Enhanced enzyme production from mixed cultures of *Trichoderma reesei* RUT-C30 and *Aspergillus niger* LMA grown as fed batch in a stirred tank bioreactor. *Biochem Eng J* 42:41–46
- Al-Zuhair S (2008) The effect of crystallinity of cellulose on the rate of reducing sugars production by heterogeneous enzymatic hydrolysis. *Bioresour Techn* 99:4078–4085
- Atalla RH, VanderHart DL (1984) Native cellulose: a composite of two distinct crystalline forms. *Science* 223:283–285
- Azizi Samir MAS, Alloin F, Dufresne A (2005) Review of recent research into cellulosic whiskers, their properties and their application in nanocomposite field. *Biomacromol* 6(2):612–626
- Bansal P, Hall M, Realf MJ, Lee JH, Bommarius AS (2010) Multivariate statistical analysis of X-ray data from cellulose: a new method to determine degree of crystallinity and predict hydrolysis rates. *Bioresour Tech* 101:4461–4471
- Ciolacu D (2007) On the supramolecular structure of cellulose allomorphs after enzymatic degradation. *J Optoelectron Adv Mater* 9(4):1033–1037
- Ciolacu D, Popa VI (2010a) Cellulose allomorphs: structure, accessibility and reactivity, series: polymer science and technology. Nova Science Publishers, Inc., United States
- Ciolacu D, Popa VI (2010b) Cellulose allomorphs—overview and perspectives. In: Lejeune A, Deprez T (eds) *Cellulose: structure and properties, derivatives and industrial uses*. Nova Science Publishers, Inc., United States, pp 1–38
- Ciolacu D, Ciolacu F, Dumitriu R, Vasile C, Popa VI (2007) Kinetics aspects in the enzymatic hydrolysis of cellulose allomorphs. *Cellulose Chem Tech* 41(1):35–40



- Ciolacu D, Ciolacu F, Popa VI (2008) Supramolecular structure—a key parameter for cellulose biodegradation. *Macromol Symp* 272(1):136–142
- Das K, Ray D, Bandyopadhyay NR, Sengupta S (2010) Study of the properties of microcrystalline cellulose particles from different renewable resources by XRD, FTIR, nanoindentation, TGA and SEM. *J Polym Environ* 18:355–363
- Davies G, Henrissat B (1995) Structures and mechanisms of glycosyl hydrolases. *Structure* 3(9):853–859
- Garvey CJ, Parker IH, Simon GP (2005) On the interpretation of X-ray diffraction powder patterns in terms of the nanostructure of cellulose I fibres. *Macromol Chem Phys* 206:1568–1575
- Gusakov AV, Salanovich TN, Antonov AI, Usti-nov BB, Okunev ON, Burlingame R, Emalfarb M, Baez M, Sinityn AP (2007) Design of highly efficient cellulase mixtures for enzymatic hydrolysis of cellulose. *Biotechnol Bioeng* 97:1028–1038
- Habibi Y, Lucia LA, Rojas OJ (2010) Cellulose nanocrystals: chemistry, self-assembly, and applications. *Chem Rev* 110(6):3479–3500
- Hayashia N, Sugiyama J, Okano T, Ishihara M (1997) The enzymatic susceptibility of cellulose microfibrils of the algal-bacterial type and the cotton-ramie type. *Carbohydr Res* 305(2):261–269
- Hu XP, Hsieh YL (1996) Crystalline structure of developing cotton fibers. *J Polym Sci B Polym Phys* 34:1451–1459
- Karmakar M, Ray RR (2011) Current trends in research and application of microbial cellulases. *Res J Microbiol* 6:41–53
- Krässig HA (1993) Methods of fiber structure characterization. In: Huglin MB (ed) *Cellulose: structure, accessibility and reactivity, polymer monographs, vol 11, chapter 3*. Gordon and Breach Science Publishers, Philadelphia, pp 43–149
- Kumar R, Singh S, Singh OV (2008) Bioconversion of lignocellulosic biomass: biochemical and molecular perspectives. *J Ind Microbiol Biotechnol* 35:377–391
- Liu H, Fu SY, Zhu JY, Li H, Zhan HY (2009) Visualization of enzymatic hydrolysis of cellulose using AFM phase imaging. *Enzyme Microb Technol* 45:274–281
- Lyagin E, Drews A, Bhattacharya S, Kraume M (2011) Continuous membrane-based screening system for biocatalysis. *Membranes* 1:70–79
- Lynd LR, Weimer PJ, van Zyl WH, Pretorius IS (2002) Microbial cellulose utilization: fundamentals and biotechnology. *Microbiol Mol Biol Rev* 66:506
- MacLellan J (2010) Strategies to enhance enzymatic hydrolysis of cellulose in lignocellulosic biomass. *MMG 445 Basic Biotech e-J* 6:31–35
- Mansfield SD, Meder R (2003) Cellulose hydrolysis—the role of monocomponent cellulases in crystalline cellulose degradation. *Cellulose* 10:159–169
- Miller GL (1959) Use of dinitrosalicylic acid reagent for determination of reducing sugar. *Anal Chem* 31(3):426–428
- Mussatto SI, Fernandes M, Milagres AMF, Roberto IC (2008) Effect of hemicellulose and lignin on enzymatic hydrolysis of cellulose from brewer's spent grain. *Enz Microb Tech* 43:124–129
- Nishiyama Y, Langan P, Chanzy H (2002) Crystal structure and hydrogen-bonding system in cellulose I $\beta$  from synchrotron X-ray and neutron fiber diffraction. *J Am Chem Soc* 124:9074–9082
- Nishiyama Y, Sugiyama J, Chanzy H, Langan P (2003) Crystal structure and hydrogen bonding system in cellulose I $\alpha$  from synchrotron X-ray and neutron fiber diffraction. *J Am Chem Soc* 125:14300–14306
- Paakko M, Ankerfors M, Kosonen H, Nykanen A, Ahola S, Osterberg M, Ruokolainen J, Laine J, Larsson PT, Ikkala O, Lindstrom T (2007) Enzymatic hydrolysis combined with mechanical shearing and high-pressure homogenization for nanoscale cellulose fibrils and strong gels. *Bio-macromol* 8:1934–1941
- Pu Y, Ziemer C, Ragauskas AJ (2006) CP/MAS <sup>13</sup>C NMR analysis of cellulase treated bleached softwood kraft pulp. *Carbohydr Res* 341(5):591–597
- Russell JB, Muck RE, Weimer PJ (2009) Quantitative analysis of cellulose degradation and growth of cellulolytic bacteria in the rumen. *FEMS Microbiol Ecol* 67(2):183–197
- Siqueira G, Tapin-Lingua S, Bras J, da Silva Perez D, Dufresne A (2010) Morphological investigation of nanoparticles obtained from combined mechanical shearing, and enzymatic and acid hydrolysis of sisal fibers. *Cellulose* 17:1147–1158
- Siró I, Plackett D (2010) Microfibrillated cellulose and nanocomposite materials: a review. *Cellulose* 17(3):459–494
- Sun Y, Zhuang J, Lin L, Ouyang P (2009) Clean conversion of cellulose into fermentable glucose. *Biotech Adv* 27:625–632
- Varma AJ (2004) Biodegradable polymers from renewable forest resources. In: Smith R (ed) *Biodegradable polymers for industrial applications*. Woodhead Publishing Limited, Cambridge, p 223
- Wada M, Chanzy H, Nishiyama Y, Langan P (2004a) Cellulose III $\alpha$  crystal structure and hydrogen bonding by synchrotron X-ray and neutron fiber diffraction. *Macromol* 37(23):8548–8555
- Wada M, Heux L, Sugiyama J (2004b) Polymorphism of cellulose I family: reinvestigation of cellulose IV $\alpha$ . *Biomacromol* 5:1385–1391
- Wada M, Nishiyama Y, Langan P (2006) X-ray structure of ammonia-cellulose I: new insights into the conversion of cellulose I to cellulose III $\alpha$ . *Macromol* 39(8):2947–2952
- Wada M, Ike M, Tokuyasu K (2010) Enzymatic hydrolysis of cellulose I is greatly accelerated via its conversion to the cellulose II hydrate form. *Polym Degrad Stab* 95:543–548
- Weimer PJ, Odt CL (1995) Cellulose degradation by ruminant microbes: physiological and hydrolytic diversity among ruminant cellulolytic bacteria. In: Sandler JN, Penner MH (eds) *Enzymatic degradation of insoluble carbohydrates*, chapter 18. ACS symposium series, vol 618, pp 291–304
- Yeh AI, Huang YC, Chen SH (2010) Effect of particle size on the rate of enzymatic hydrolysis of cellulose. *Carbohydr Polym* 79:192–199
- Zhang YHP, Lynd LR (2004) Toward an aggregated understanding of enzymatic hydrolysis of cellulose: noncomplexed cellulase systems. *Biotechnol Bioeng* 88(7):797–824